Labeling nanoparticles – dye leakage and altered cellular uptake

Sofie Snipstad[1], Sjoerd Hak[1,2], Habib Baghirov[1], Einar Sulheim[1,3], Yrr Mørch[3], Sylvie Lelu[1], Eva von Haartman[4,5], Marcus Bäck[6], K. Peter R. Nilsson[6], Andrey S. Klymchenko[7], Catharina de Lange Davies[1], Andreas K. O. Åslund[1]

[1] Department of Physics, The Norwegian University of Science and Technology, Trondheim, Norway

[2] Department of Circulation and Medical Imaging, The Norwegian University of Science and Technology, Trondheim, Norway

[3] SINTEF Materials and Chemistry, Trondheim, Norway

[4] Pharmaceutical Sciences Laboratory, Åbo Akademi University, Turku, Finland

[5] Laboratory of Physical Chemistry, Åbo Akademi University, Turku, Finland

[6] Department of Physics, Chemistry and Biology, Linköping University, Linköping, Sweden

[7] Laboratoire de Biophotonique et Pharmacologie, UMR CNRS 7213, Université de Strasbourg, Strasbourg, France

Abstract

I*n vitro* and *in vivo* behavior of nanoparticles (NPs) is often studied by tracing the NPs with fluorescent dyes. This requires stable incorporation of dyes within the NPs, as dye leakage may give a wrong interpretation of NP biodistribution, cellular uptake and intracellular distribution. Furthermore, NP labeling with trace amounts of dye should not alter NP properties such as interactions with cells or tissues.

To allow for versatile NP studies with a variety of fluorescence-based assays, labeling of NPs with different dyes is desirable. Hence, when new dyes are introduced, simple and fast screening methods to assess labeling stability and NP-cell interactions are needed. For this purpose we have used a previously described generic flow cytometry assay; incubation of cells with NPs at 4°C and 37°C. Cell-NP interaction is confirmed by cellular fluorescence after 37°C incubation, and NP dye retention is confirmed when no cellular fluorescence is detected at 4°C.

Three different NP-platforms labeled with six different dyes were screened, and a great variability in dye retention was observed. Surprisingly, incorporation of trace amounts of certain dyes was found to reduce, or even inhibit NP uptake. This work highlights the importance of thoroughly evaluating every dye-NP combination before pursuing fluorescent NP applications.

Keywords: Polymeric nanoparticles, nanoemulsions, liposomes, leakage, cellular uptake, flow cytometry

Running header: Labeling nanoparticles

Corresponding author: Andreas Åslund, Høyskoleringen 5, 7491 Trondheim, +4745390137, andreas.aslund@ntnu.no

Acknowledgements:

Anne Rein Hatletveit, Lars Erik Parnas, Sidsel Sundseth and Kristin Grendstad Sæterbø are acknowledged for technical support. Henkel Loctite, Cremer and Huntsman have kindly provided cyanoacrylate, Miglyol and Jeffamine, respectively. The research was funded by The Central Norway Regional Health Authority and The Research Council of Norway (NANO2021 project number 220005 and BIOTEK2021 project number 226159).

Conflict of interest:

The authors declare no conflict of interest.

Introduction

Nanotechnology has enabled development of multifunctional nanoparticles (NPs) for various medical applications. Improved diagnostics and therapy of various diseases has been achieved by incorporating contrast agents for imaging and drugs for therapy (1-5). In order to understand the behavior of NPs *in vitro* and *in vivo* it is necessary to trace them. This is commonly done by encapsulation of fluorescent dyes in the NPs, which allows their detection with optical techniques (6-12). Encapsulating dyes and drugs in NPs might change the properties both of the NPs and the encapsulated molecules. This could modify surface properties (13) and change the NP charge (14) and interaction between the NPs and other molecules and cells. It is well known that changing the size, shape or surface charge of NPs can alter the NP uptake in cells (15-17). Furthermore, the NP and the fluorescent probe do not always behave as a single unit; various examples of leakage of dyes from NPs have been reported (18-21). Fluorescence from released dyes can wrongly be interpreted as NP-fluorescence, causing the apparent cellular uptake, intracellular distribution, and biodistribution to not represent that of the NPs (18,22-24). This emphasizes the importance of choosing a fluorescent dye that is compatible with the NP-platform into which it is incorporated. Various procedures have been developed to evaluate NP-labeling stability (18,20,23,25-29). However, the majority of these assays do not include cells or serum, which could strongly affect dye release as these serve as acceptor compartments for released dye *in vivo* (18,24,29-33).

We have previously shown that Nile Red (NR) leaks out of poly(butyl cyanoacrylate) (PBCA)-NPs upon cell contact (24), which is in line with various studies showing NR release from NPs (18,19,25,26). The hydrophobic analogue NR668 was found to leak much less than NR from nanoemulsions (NEs) (18), and to be suitable for tracing the PBCA-NPs, as it was not released from the NPs until they were endocytosed and degraded (12). In search of

alternative dyes for stable NP labeling and potential Förster resonance energy transfer (FRET) pairs, we performed the current study and applied a flow cytometric cell based assay to screen a variety of dye-NP combinations. Cells were incubated with NPs at 4°C or 37°C, and cellular binding and uptake of dyes or NPs were quantified by flow cytometry (FCM). Energy depletion at 4°C (20,23) was used to determine whether cellular uptake was active or passive (22,34,35). Energy dependent uptake (28,36) is likely the main mechanism for internalization of NPs. Thus, lack of fluorescence at 4°C indicates no leakage of the dye from the NP, whereas cellular fluorescence at 4°C might be due to dye leakage and subsequent energy-independent transfer of the dye to the cell, or due to cell surface-associated NPs. No fluorescence at 37°C indicates lack of NP uptake, and the enhanced fluorescence from incubation at 4°C to 37°C results mainly from NPs being endocytosed (37) or associated with the plasma membrane (38). Thus, the assay provides information both about dye retention in NPs as well as how labeling NPs affects their association with and uptake by cells. Two different cell lines, with different propensities to take up PBCA-NPs (12), were used. The rat brain endothelial cell line RBE4 was chosen because of the reported ability of PBCA-NPs to cross the blood brain barrier (39), and the human prostate cancer cell line PC3 was chosen because it is a widely used cancer cell line.

Six different hydrophobic fluorophores (Figure 1) encapsulated in three commonly used NP-platforms – PBCA-NPs, NEs and liposomes – were studied systematically. Hydrophobic dyes are often used as models for hydrophobic drugs, which due to their low solubility in water, benefit from encapsulation in a nanocarrier. Three of these dyes – NR, DiI and DiD (Figure 1) – are commercially available and commonly used for NP encapsulation. The other dyes were synthesized; NR668 designed to be more hydrophobic than NR, the oligothiophene p-HTAM has been used in a previous study of cellular uptake of NPs (12), and similarly to NR668, p-HTAH was designed to be more hydrophobic than p-HTAM. We

demonstrate a large variability in NP-dye retention, and surprisingly found that encapsulation of different dyes significantly alters NP uptake in cells.

Materials and methods

Cell cultures

Human prostate adenocarcinoma cells (PC3, American Type Culture Collection, CRL-1435, Manassas, USA) were cultured in Dulbecco's modified Eagle's medium (DMEM, Gibco, Thermo Fischer Scientific, Waltham, USA) supplemented with 10% fetal bovine serum (FBS, Sigma-Aldrich, St Louis, USA) at 37°C and 5% CO_2.

Rat brain endothelial cells (RBE4, a kind gift from Dr. Aschner, Vanderbilt University, Nashville, USA) were cultured at 37°C and 5% CO_2 in 1:1 mix of Ham's F-10 medium and MEM medium (both from Thermo Fischer Scientific) supplemented with 10% fetal bovine serum, 300 μg/ml G418 and 1 ng/ml basic fibroblast growth factor (Thermo Fischer Scientific).

Dyes used to label NPs

NR (Sigma-Aldrich, catalogue number 72485), NR668 (18), p-HTAM (40), p-HTAH, DiI and DiD (last two from Thermo Fischer Scientific, catalogue numbers D-7757 and D-282 respectively) were encapsulated in NPs. The structures of the different dyes are shown in Figure 1, along with their emission spectra in NPs at the excitation wavelengths used for FCM.

Synthesis of p-HTAH

See supplementary information and Supplementary Scheme 1.

Synthesis of polymeric- and lipid-based NPs

PBCA-NPs were synthesized by the miniemulsion process as described previously (41) and presented in Supplementary information. Oil-in-water NEs were prepared as described previously (42) and presented in Supplementary information. Liposomes were prepared as the NEs, with the following differences: no soybean oil was added, and the sonication time was only 10 min.

Characterization of the NPs

The NPs were characterized for size and polydispersity index (PDI) using dynamic and electrophoretic light scattering (Zetasizer Nano ZS, Malvern Instruments, Westborough, USA) in 0.01M phosphate buffer, pH 7. Surface charge (zeta-potential) was measured for the various PBCA-NPs.

To verify successful labeling of NPs, a spectrophotometer (Tecan Infinite 200Pro, Männedorf, Switzerland) was used to measure the fluorescence spectra from NPs in deionized water (20 μg/ml of PBCA for NPs, 76 μg/ml amphiphilic lipid for liposomes and NEs) at the excitation wavelengths used in FCM.

Incubation with cells

125 000 PC3 cells (passage 40-70) were seeded in 12-well plates (Corning, Corning, USA). 48 h later the medium was changed, and at 72 h the medium was replaced with medium containing 20 μg/ml PBCA-NPs or 76 μg/ml amphiphilic lipid for NEs and liposomes. The cells were incubated at 37°C or 4°C for 3 h. The cells at 4°C were pre-incubated at 4°C for 15 min before addition of NPs. Before FCM, the cells were washed with PBS (4°C or 37°C) 3 times to remove surface-associated NPs, trypsinized, resuspended in 4°C medium and placed on ice.

To study association with RBE4 cells, 100 000 cells (passage 14-18) were seeded in 12-well plates (Corning). 48 h after seeding, the medium was changed to medium containing PBCA-NPs, NEs or liposomes at concentrations given above, and the cells were prepared for FCM after 3 h incubation as described above, except that no incubation at 4°C was performed.

For co-incubation of cells with NPs and free dyes, PC3 and RBE4 cells were co-incubated with either DiI dye and PBCA-NPs containing p-HTAM or with P-HTAH dye and PBCA-NPs containing NR668 for 3 h at 37°C, and the cells were prepared for FCM as described above. Cells were also incubated with the free dyes only. Concentrations of free dyes were similar to the amount of dye incorporated in NEs/liposomes.

Quantification by FCM

Fluorescence from cells was measured using FCM (Beckman Coulter Gallios, Fullerton, USA). NR and NR668 were excited at 561 nm and fluorescence was detected at 620 nm using a 30 nm bandpass filter. p-HTAM and p-HTAH were excited at 405 nm and fluorescence was detected at 450 nm using a 50 nm bandpass filter. DiD was excited at 633 nm and fluorescence was detected at 660 nm using a 20 nm bandpass filter, while DiI was excited at 561 nm and detected at 582 nm with a 15 nm bandpass filter.

A minimum of 10 000 cells were counted per sample, and cellular fragments and debris were excluded from the analysis by subjectively choosing a collection gate from the distribution in the side-scatter versus forward-scatter dot plot (an example is shown in Supplementary Figure 1). The data were analyzed using Kaluza Flow Cytometry Analysis software v1.2 (Beckman Coulter). Additional FCM details are presented in the Supplementary information.

Results

The range of sizes and PDIs of the PBCA-NPs, NEs and liposomes are presented in Table 1. All the NPs were successfully fluorescently labeled (Supplementary Table 1). Zeta-potential of the various PBCA-NPs were -2 to -4 mV.

Dye retention in NPs

FCM analysis of PC3 cells incubated with the various NPs at 4°C showed that dye retention varied greatly between the various dyes and NPs studied (Figure 2A). In general, dyes were more stably incorporated in PBCA-NPs than in lipid-based NPs. The results are summarized in Table 2.

NR leaked out of all three NP platforms. The cellular fluorescence was almost the same at 4°C and 37°C, indicating extensive NR release from the NPs, in accordance with our previously reported study of PBCA-NPs (24) and NEs (18). The hydrophobic analogue of NR, NR668 (12,18), was retained within the PBCA-NPs, but for the lipid-based NPs some leakage was observed. The commonly used lipophilic carbocyanines, DiI and DiD, were retained within all three NP-platforms as no cellular fluorescence was detected at 4°C. p-HTAM was retained in PBCA-NPs and NEs, but some leakage from liposomes was observed. Incubation using our newly synthesized oligothiophene, p-HTAH, which has hexane alkyl chains instead of methyl like p-HTAM, did not show any cellular fluorescence at 4°C, indicating that the dye is retained in the NPs. Surprisingly, no cellular fluorescence was detected at 37°C either, and free p-HTAH did not stain cells (data not shown).

Dye encapsulation can prevent cellular NP uptake

The uptake of p-HTAH-NPs in PC3 cells was inhibited compared to those with p-HTAM. Similar to NPs with p-HTAH, NEs labeled with the two carbocyanines and liposomes labeled with DiI did not show cellular fluorescence at 37°C either (Figure 2A). We have also found that PBCA-NPs encapsulating DiO were not taken up at 37°C (Supplementary Figure 2). NR668 and p-HTAM encapsulated in all three NPs as well as DiI and DiD in PBCA-NPs and DiD in liposomes showed higher cellular fluorescence at 37°C than 4°C, indicating endocytosis and/or surface binding of the NPs (Table 3, Figure 2A).

To further study the lack of cellular uptake of the various NPs at 37°C, RBE4 cells which internalizes PBCA-NP more efficiently than PC3 cells (12), were included. All PBCA-NPs, including those with encapsulated p-HTAH, showed RBE4 cell-association (Table 3, Figure 2B). However, the uptake of p-HTAH-PBCA-NPs was reduced compared to p-HTAM-PBCA-NPs, even though p-HTAH-PBCA-NPs showed higher fluorescence intensity (Supplementary Table 1). For liposomes and NEs, however, the association with RBE4 cells varied depending on the dye. NEs and liposomes labeled with NR668, p-HTAM or p-HTAH all showed cellular fluorescence at 37°C. In accordance with results from PC3 cells, RBE4 cells showed hardly any cellular fluorescence after incubation at 37°C with neither NEs nor liposomes labeled with DiI or NEs labeled with DiD.

To investigate whether the lack of fluorescence in PC3 cells incubated with p-HTAH encapsulated in PBCA-NPs was due to NPs not being endocytosed, PC3 and RBE4 cells were incubated at 37°C with PBCA-NPs labeled with both p-HTAH and NR668. No fluorescence from either dye was detected by FCM in PC3 cells, but both fluorophores were detected in RBE4 (Figure 2C and 2D, respectively). This strengthened the indication that p-HTAH prevented NPs from being taken up in PC3 cells.

Furthermore, PC3 cells were co-incubated at 37°C with one NP shown to be cell-associated and one NP that was not. The combinations used were NEs or liposomes with DiI (no cell-association) together with PBCA-NPs containing p-HTAM (cell-association), and NEs or liposomes with p-HTAH (no cell-association) together with PBCA-NPs containing NR668 (cell-association). Only the combination of DiI liposomes and PBCA-NPs with p-HTAM showed cellular fluorescence from PBCA-NPs. NEs with DiI and NEs/liposomes with p-HTAH thus prevented cellular association of both NR668 as well as p-HTAM labeled PBCA-NPs (Supplementary Figure 3A). Interestingly, free DiI and p-HTAH did not affect cellular association of PBCA-NPs in co-incubation experiments (Supplementary Figure 3B and C).

Discussion

In the current study, a rapid FCM-based screening method was used to evaluate the retention of six different dyes in three different NP-platforms. Various approaches are reported in the literature to determine leakage of fluorescent dyes from NPs (12,18,20,23-29). Several studies are based on *in vitro* dye/drug release in aqueous solution by separation methods (25). Others have used lipid acceptor compartments to evaluate the dye's propensity to leak out of the NP (25-27). We chose to use a simple cell based FCM assay which can be used with a wide variety of cell lines (20,22,24). The advantage of using FCM is that it is a rapid and quantitative method allowing screening of a large number of samples. A limitation is that the method does not separate fluorescence from internalized and surface-bound dyes or NPs (43). Thus additional methods are needed to verify whether the NPs are internalized. Microscopy is another method used for studying uptake and distribution of NPs (18,22,37,43). However, microscopy should be employed with care in the assessment of dye leakage, as free hydrophobic dyes will bind to intracellular hydrophobic molecules resulting in both diffuse and spotted staining pattern (12,24,30,33), thereby making the dye hard to separate from the

fluorescence of intact NPs. In a previous study, we have shown that PBCA-NPs with NR668 are taken up in PC3 cells by endocytosis, verified by the use of time consuming intracellular spectral microscopy and fluorescence-lifetime imaging microscopy (FLIM) (12). This illustrates that although highly useful, microscopy is not suitable for rapid screening of a large number of samples. In several other studies, FRET has been used to study release from NPs (18,21,28). Although this represents an elegant approach, and allows for real-time *in vivo* follow up of dye release, it requires successful incorporation of two dyes, one donor and one acceptor, and extensive optimization and control experiments.

Dye retention and leakage from NPs

In the current study, some dyes were found to be retained in the NPs (NR668 for PBCA-NPs, p-HTAM for PBCA-NPs and NEs, and DiD and DiI in all NPs). In case of the other fluorophores (NR for all NPs, NR668 for NEs and liposomes and p-HTAM for liposomes) dye leakage could not be ruled out. These results demonstrate that dye retention is highly dependent on both dye and NP-platform, and that thorough evaluation of labeling stability is critical.

When no fluorescence was observed at 4°C, we concluded that the dyes are retained in the NPs. This is correct when the assumption that free dyes would enter the cells via energy independent processes holds. The free dyes NR, NR668 and p-HTAM have indeed been confirmed to stain cells in our previous work using microscopy (12,24). In addition, DiD and DiI are known to diffuse across the plasma membrane (28,44,45). Thus, DiI and DiD in NEs and liposomes are most likely retained, as any leakage of the dyes from NPs would presumably stain the cells. However, free p-HTAH was not found to label cells it is possible

that not even a DMSO formulation is enough to solubilize the very hydrophobic p-HTAH in aqueous solutions, thus retention of this fluorophore by the NPs is uncertain.

The problem of fluorophore leakage has also been recognized by others, and their observations are largely in agreement with our results (18,19,21,22,25,26,28,46-48). NR has repeatedly been shown to leak out of various NPs (18,19,25,26), and we concluded in a previous study that NR was taken up by cells through contact-mediated transfer within minutes after addition of PBCA-NPs (24). The retention of a dye in a NP is largely governed by hydrophobic and electrostatic interaction between the dye and NP. Its compatibility with the hydrophobic phase in the NPs (polymer core in the case of PBCA-NPs, oil core and phospholipid monolayer in the case of NE, and phospholipid bilayer in the case of liposomes) plays an important role in dye release. For dyes which do not leak from the NPs, the dye is likely to have a strong preference for the hydrophobic phase and to be confined within the hydrophobic compartment. Thus, it is not released from the NP until the NP degrades. A dye that is not retained efficiently is presumably more present at the NP-surface as compared to non-leaky dyes (18). Accordingly, these dyes are present in the shell of the NP, and a continuous release not associated with NP-degradation may occur.

Dye encapsulation can prevent cellular NP uptake

Studying cellular uptake of NPs is commonly done by labeling the NPs with fluorescent dyes. In accordance with this practice, we studied uptake of PBCA-NP in PC3 and RBE4 cells and to our surprise found that when encapsulating some dyes no cellular uptake was detected. Thus we performed the systematic study presented here. Both the carbocyanines DiI and DiD and the oligothiophene p-HTAH inhibited cellular uptake of NPs. To further study this

inhibition we encapsulated both NR668 (that is taken up by PC3-cells) and p-HTAH (that is not taken up) in PBCA-NP. As a result, the NP was not taken up in PC3 cells, however, a clear uptake in RBE4 was still detected, in accordance with the uptake behavior of the individually encapsulated dyes. Next, PC3 cells were co-incubated with a NP that was taken up and one that was not. In three out of the four combinations, uptake of the NPs was inhibited by the NP-dye that inhibits uptake. The mechanisms underlying the observed effect are not clear. The reduced cellular uptake was not due to the size or zetapotential of the NPs; the encapsulation of the dyes did not change the size of the NPs significantly, and for all the PBCA-NPs the zetapotential was -2 to -4 mV.

The chemical composition and structure of the encapsulated dye might affect the cellular uptake. The common denominators for NP-encapsulated dyes that inhibit cellular uptake are long alkyl chains (hexyl or longer) and quartenary amines. However, NR668 has both these functionalities but did not inhibit cellular uptake of NPs. The carbocyanines on the other hand, having quartenary amines, inhibited cellular uptake of lipid based NPs. This inhibition also depended on the interaction with the NPs, as cellular uptake of liposomes with DiD was not inhibited. To fully elucidate how the NP-interaction with the cell changes upon a change of dyes would require a more thorough study of both the NP chemistry and the processes involved in endocytosis.

Conclusions

A systematic study of different hydrophobic dyes encapsulated in three different NP-platforms has been performed. Dye retention was found to vary greatly between the various dyes and NPs studied. Moreover, we have shown that the choice of dye may also impact the uptake behavior of the NP. The implications of our observations are significant for anyone

that is studying the properties of NPs with fluorescence-based methods, or when trace amounts of a fluorophore are replaced with high payloads of drugs for drug delivery purposes. Our findings highlight the importance of evaluating every combination of encapsulated agent and NP-platform before making conclusions about interactions with cells and tissue or payload release.

References

1. Murthy SK. Nanoparticles in modern medicine: state of the art and future challenges. Int J Nanomedicine 2007;2:129-41.
2. Naahidi S, Jafari M, Edalat F, Raymond K, Khademhosseini A, Chen P. Biocompatibility of engineered nanoparticles for drug delivery. J Control Release 2013;166:182-94.
3. Salata O. Applications of nanoparticles in biology and medicine. J Nanobiotechnology 2004;2:3.
4. Etheridge ML, Campbell SA, Erdman AG, Haynes CL, Wolf SM, McCullough J. The big picture on nanomedicine: the state of investigational and approved nanomedicine products. Nanomedicine 2013;9:1-14.
5. Skotland T, Iversen TG, Sandvig K. Development of nanoparticles for clinical use. Nanomedicine 2014;9:1295-1299.
6. Licha K, Olbrich C. Optical imaging in drug discovery and diagnostic applications. Adv Drug Deliv Rev 2005;57:1087-108.
7. Sokolova V, Epple M. Synthetic pathways to make nanoparticles fluorescent. Nanoscale 2011;3:1957-1962.
8. Elsabahy M, Wooley KL. Design of polymeric nanoparticles for biomedical delivery applications. Chem Soc Rev 2012;41:2545-2561.
9. Liong M, Lu J, Kovochich M, Xia T, Ruehm SG, Nel AE, Tamanoi F, Zink JI. Multifunctional inorganic nanoparticles for imaging, targeting, and drug delivery. ACS Nano 2008;2:889-96.
10. Torchilin VP. Fluorescence microscopy to follow the targeting of liposomes and micelles to cells and their intracellular fate. Adv Drug Deliv Rev 2005;57:95-109.
11. Hak S, Helgesen E, Hektoen HH, Huuse EM, Jarzyna PA, Mulder WJ, Haraldseth O, Davies C de L. The effect of nanoparticle polyethylene glycol surface density on ligand-directed tumor targeting studied in vivo by dual modality imaging. ACS Nano 2012;6:5648-58.
12. Sulheim E, Baghirov H, von Haartman E, Bøe A, Åslund AK, Mørch Y, Davies CdL. Cellular uptake and intracellular degradation of poly(alkyl cyanoacrylate) nanoparticles. Journal of Nanobiotechnology;DOI: 10.1186/s12951-015-0156-7.
13. Panyam J, Labhasetwar V. Biodegradable nanoparticles for drug and gene delivery to cells and tissue. Adv Drug Deliv Rev 2003;55:329-47.
14. Sahoo SK, Panyam J, Prabha S, Labhasetwar V. Residual polyvinyl alcohol associated with poly (D,L-lactide-co-glycolide) nanoparticles affects their physical properties and cellular uptake. J Control Release 2002;82:105-14.
15. He C, Hu Y, Yin L, Tang C, Yin C. Effects of particle size and surface charge on cellular uptake and biodistribution of polymeric nanoparticles. Biomaterials 2010;31:3657-66.
16. Champion JA, Katare YK, Mitragotri S. Particle shape: a new design parameter for micro- and nanoscale drug delivery carriers. J Control Release 2007;121:3-9.
17. Ma N, Ma C, Li C, Wang T, Tang Y, Wang H, Moul X, Chen Z, Hel N. Influence of nanoparticle shape, size, and surface functionalization on cellular uptake. J Nanosci Nanotechnol 2013;13:6485-98.
18. Klymchenko AS, Roger E, Anton N, Anton H, Shulov I, Vermot J, Mely Y, Vandamme TF. Highly lipophilic fluorescent dyes in nano-emulsions: towards bright non-leaking nano-droplets. Rsc Adv 2012;2:11876-11886.
19. Xu P, Gullotti E, Tong L, Highley CB, Errabelli DR, Hasan T, Cheng JX, Kohane DS, Yeo Y. Intracellular drug delivery by poly(lactic-co-glycolic acid) nanoparticles, revisited. Mol Pharm 2009;6:190-201.
20. Andreozzi P, Martinelli C, Carney RP, Carney TM, Stellacci F. Erythrocyte Incubation as a Method for Free-Dye Presence Determination in Fluorescently Labeled Nanoparticles. Mol Pharmaceut 2013;10:875-882.

21. Simonsson C, Bastiat G, Pitorre M, Klymchenko AS, Bejaud J, Mely Y, Benoit JP. Inter-nanocarrier and nanocarrier-to-cell transfer assays demonstrate the risk of an immediate unloading of dye from labeled lipid nanocapsules. Eur J Pharm Biopharm 2016;98:47-56.
22. Salvati A, Aberg C, dos Santos T, Varela J, Pinto P, Lynch I, Dawson KA. Experimental and theoretical comparison of intracellular import of polymeric nanoparticles and small molecules: toward models of uptake kinetics. Nanomedicine 2011;7:818-26.
23. Tenuta T, Monopoli MP, Kim J, Salvati A, Dawson KA, Sandin P, Lynch I. Elution of labile fluorescent dye from nanoparticles during biological use. PLoS One 2011;6:e25556.
24. Snipstad S, Westrøm S, Mørch Y, Afadzi M, Åslund AK, Davies CdL. Contact-mediated intracellular delivery of hydrophobic drugs from polymeric nanoparticles. Cancer Nanotechnol 2014;5.
25. Petersen S, Fahr A, Bunjes H. Flow Cytometry as a New Approach To Investigate Drug Transfer between Lipid Particles. Mol Pharm 2010;7:350-363.
26. Bastiat G, Pritz CO, Roider C, Fouchet F, Lignieres E, Jesacher A, Glueckert R, Ritsch-Marte M, Schrott-Fischer A, Saulnier P and others. A new tool to ensure the fluorescent dye labeling stability of nanocarriers: a real challenge for fluorescence imaging. J Control Release 2013;170:334-42.
27. Shabbits JA, Chiu GN, Mayer LD. Development of an in vitro drug release assay that accurately predicts in vivo drug retention for liposome-based delivery systems. J Control Release 2002;84:161-70.
28. Chen HT, Kim SW, Li L, Wang SY, Park K, Cheng JX. Release of hydrophobic molecules from polymer micelles into cell membranes revealed by Forster resonance energy transfer imaging. P NATL ACAD SCI USA 2008;105:6596-6601.
29. Zhao Y, van Rooy I, Hak S, Fay F, Tang J, Davies Cde L, Skobe M, Fisher EA, Radu A, Fayad ZA and others. Near-infrared fluorescence energy transfer imaging of nanoparticle accumulation and dissociation kinetics in tumor-bearing mice. ACS Nano 2013;7:10362-70.
30. Greenspan P, Mayer EP, Fowler SD. Nile red: a selective fluorescent stain for intracellular lipid droplets. J Cell Biol 1985;100:965-73.
31. Greenspan P, Fowler SD. Spectrofluorometric Studies of the Lipid Probe, Nile Red. J Lipid Res 1985;26:781-789.
32. Skajaa T, Zhao Y, van den Heuvel DJ, Gerritsen HC, Cormode DP, Koole R, van Schooneveld MM, Post JA, Fisher EA, Fayad ZA and others. Quantum dot and Cy5.5 labeled nanoparticles to investigate lipoprotein biointeractions via Forster resonance energy transfer. Nano Lett 2010;10:5131-8.
33. Brown WJ, Sullivan TR, Greenspan P. Nile Red Staining of Lysosomal Phospholipid Inclusions. Histochemistry 1992;97:349-354.
34. Verma A, Uzun O, Hu Y, Hu Y, Han HS, Watson N, Chen S, Irvine DJ, Stellacci F. Surface-structure-regulated cell-membrane penetration by monolayer-protected nanoparticles. Nat Mater 2008;7:588-95.
35. Mahmoudi M, Abdelmonem AM, Behzadi S, Clement JH, Dutz S, Ejtehadi MR, Hartmann R, Kantner K, Linne U, Maffre P and others. Temperature: The "Ignored" Factor at the NanoBio Interface. Acs Nano 2013;7:6555-6562.
36. Dausend J, Musyanovych A, Dass M, Walther P, Schrezenmeier H, Landfester K, Mailander V. Uptake Mechanism of Oppositely Charged Fluorescent Nanoparticles in HeLa Cells. Macromol Biosci 2008;8:1135-1143.
37. Brambilla D, Nicolas J, Le Droumaguet B, Andrieux K, Marsaud V, Couraud PO, Couvreur P. Design of fluorescently tagged poly(alkyl cyanoacrylate) nanoparticles for human brain endothelial cell imaging. Chem Commun (Camb) 2010;46:2602-4.
38. Lesniak A, Salvati A, Santos-Martinez MJ, Radomski MW, Dawson KA, Aberg C. Nanoparticle Adhesion to the Cell Membrane and Its Effect on Nanoparticle Uptake Efficiency. J Am Chem Soc 2013;135:1438-1444.

39. Weiss CK, Kohnle MV, Landfester K, Hauk T, Fischer D, Schmitz-Wienke J, Mailander V. The first step into the brain: uptake of NIO-PBCA nanoparticles by endothelial cells in vitro and in vivo, and direct evidence for their blood-brain barrier permeation. ChemMedChem 2008;3:1395-403.
40. Åslund A, Sigurdson CJ, Klingstedt T, Grathwohl S, Bolmont T, Dickstein DL, Glimsdal E, Prokop S, Lindgren M, Konradsson P and others. Novel Pentameric Thiophene Derivatives for in Vitro and in Vivo Optical Imaging of a Plethora of Protein Aggregates in Cerebral Amyloidoses. ACS Chem Biol 2009;4:673–684.
41. Mørch Y, Hansen R, Berg S, Hansen Y, Åslund A, Schmid R, Kubowicz S, Johnsen H, Eggen S, Blom H and others. Nanoparticle-Stabilized Microbubbles for Multimodal Imaging and Drug Delivery. Contrast Media Mol Imaging 2015;10:356-366.
42. Jarzyna PA, Skajaa T, Gianella A, Cormode DP, Samber DD, Dickson SD, Chen W, Griffioen AW, Fayad ZA, Mulder WJ. Iron oxide core oil-in-water emulsions as a multifunctional nanoparticle platform for tumor targeting and imaging. Biomaterials 2009;30:6947-54.
43. Gottstein C, Wu GH, Wong BJ, Zasadzinski JA. Precise Quantification of Nanoparticle Internalization. ACS Nano 2013;7:4933-4945.
44. Cheng C, Trzcinski O, Doering LC. Fluorescent labeling of dendritic spines in cell cultures with the carbocyanine dye "DiI". Front Neuroanat 2014;8:30.
45. Bananis E, Nath S, Gordon K, Satir P, Stockert RJ, Murray JW, Wolkoff AW. Microtubule-dependent movement of late endocytic vesicles in vitro: requirements for Dynein and Kinesin. Mol Biol Cell 2004;15:3688-97.
46. Sun X, Li F, Wang Y, Liang W. Cellular uptake and elimination of lipophilic drug delivered by nanocarriers. Pharmazie 2010;65:737-42.
47. Hofmann D, Messerschmidt C, Bannwarth MB, Landfester K, Mailander V. Drug delivery without nanoparticle uptake: delivery by a kiss-and-run mechanism on the cell membrane. Chem Commun 2014;50:1369-1371.
48. Chan M, Schopf E, Sankaranarayanan J, Almutairi A. Iron Oxide Nanoparticle-Based Magnetic Resonance Method to Monitor Release Kinetics from Polymeric Particles with High Resolution. Analytical Chemistry 2012;84:7779-7784.

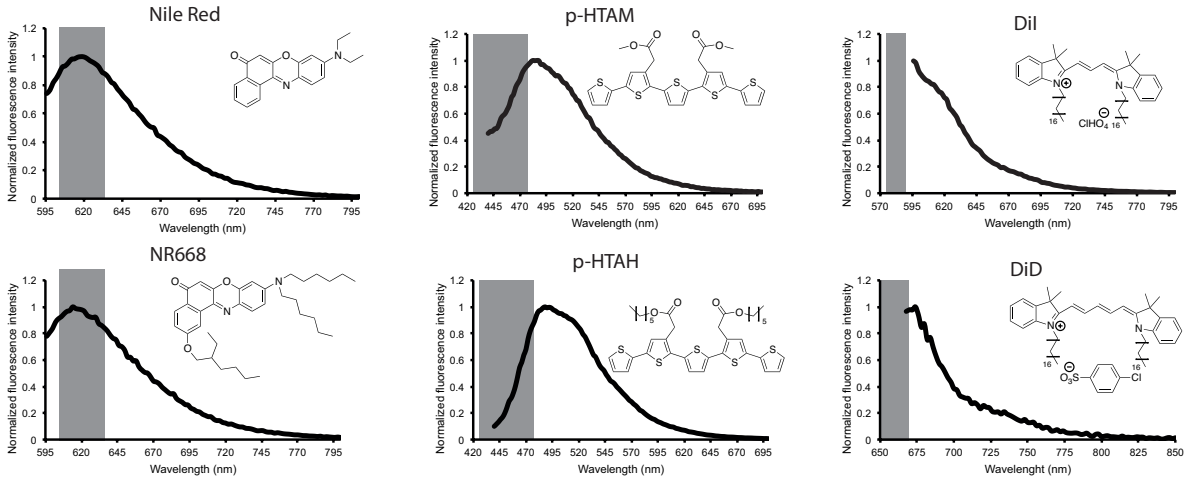

Figure 1: Chemical structures and emission spectra of the six dyes encapsulated in NPs at the excitation wavelengths used for FCM; 561 nm for NR and NR668, 405 nm for p-HTAM and p-HTAH, 561 nm for DiI and 633 nm for DiD. The detection bandpass filter used in FCM is shown in grey. The lack of overlap between the detection bandpass and spectrophotometer fluorescence spectra in some cases is due to limitations of the spectrophotometer (detection must start at least 35 nm above excitation). DiI (1,1'-dioctadecyl-3,3,3',3'-tetramethylindocarbocyanine perchlorate), DiD (1,1'-dioctadecyl-3,3,3',3'-tetramethylindodicarbocyanine 4-chlorobenzenesulfonate salt), NR668 (9-Dihexylamino-2-(2-ethyl-hexyloxy)-benzo[a]phenoxazin-5- one), p-HTAH ((3'''-carboxymethyl-[2,2';5',2'';5'',2''';5''',2''']quinquethiophen-4'-yl)-acetic acid hexyl ester) and p-HTAM ((3'''-carboxymethyl-[2,2';5',2'';5'',2''';5''',2''']quinquethiophen-4'-yl)-acetic acid methyl ester).

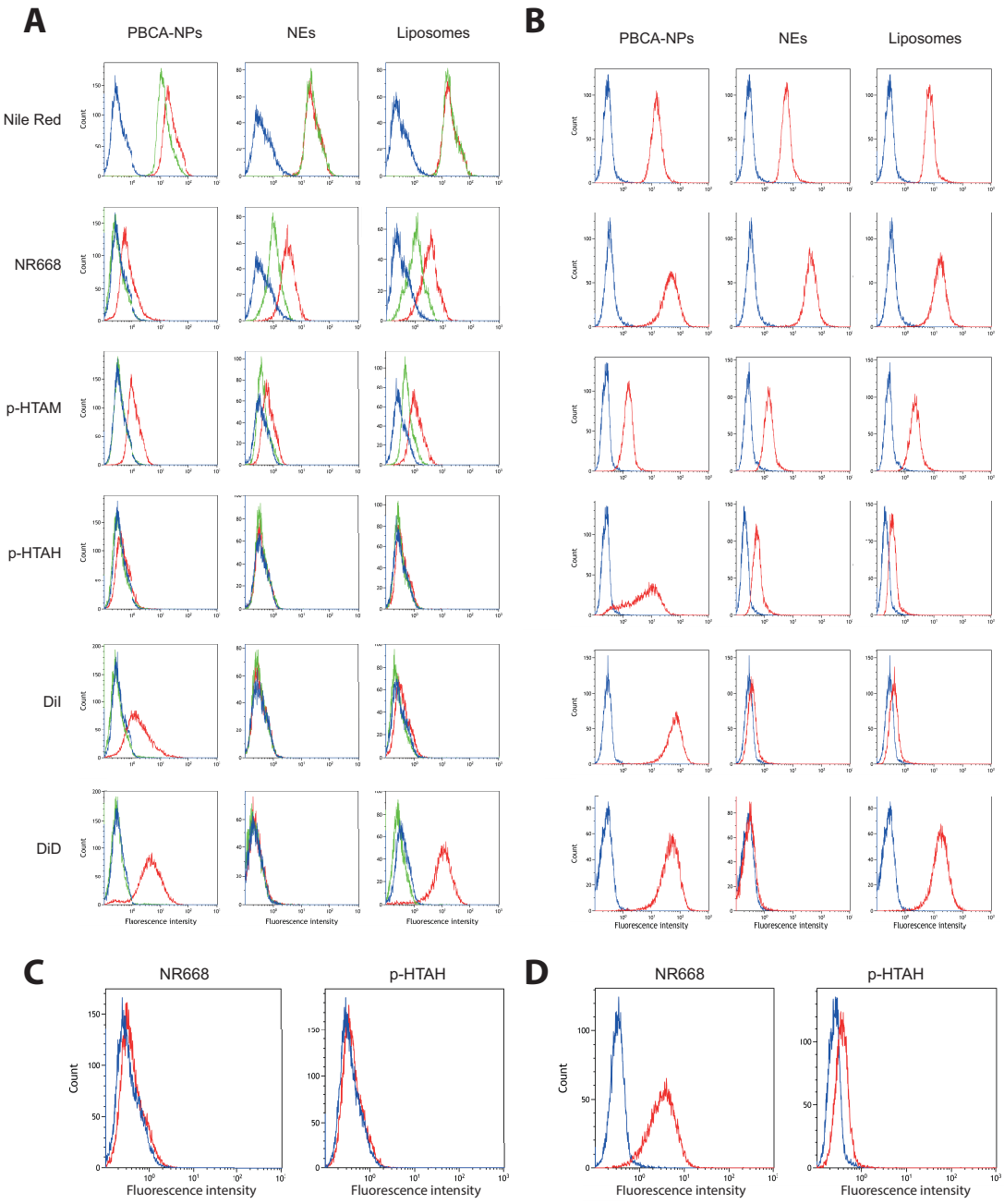

Figure 2: Flow cytometry histograms illustrating fluorescence from PC3 cells after incubation with NPs at 4°C or 37°C (**A**). The histograms show one representative experiment. All experiments were repeated 2-3 times. Flow cytometry histograms illustrating fluorescence from RBE4 cells after incubation with NPs at 37 °C (**B**). The histograms show one representative experiment. All experiments were repeated 2 times. Flow cytometry histograms illustrating association with PC3 or RBE4 cells incubated with dual-labeled (p-HTAH and NR668) PBCA-NPs at 37°C (**C** and **D** respectively). Autofluorescence (blue), incubation at 4°C (green) and incubation at 37°C (red).

Supplementary:

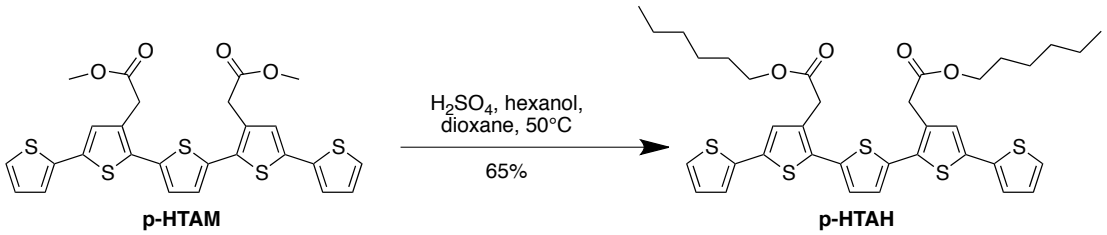

Scheme 1: Synthesis of p-HTAH.

Synthesis of p-HTAH

All chemicals were purchased from Sigma-Aldrich. p-HTAM (0.085 g, 0.153 mmol) was dissolved in dry dioxane (4 mL). Conc. H_2SO_4 (0.045 mL, 0.844 mmol) was added and the solution was heated at 50 °C overnight. The reaction was quenched with saturated $NaHCO_3$ (aq) and extracted with dichloromethane. The organic phase was dried, filtered and concentrated. Purification by high pressure liquid chromatography gave p-HTAH (0.069 g, 65%) as an orange glue. ^{1}H NMR (300 MHz, $CDCl_3$) δ 0.85 (t, J = 7.0 Hz, 6H), 1.18-1.40 (m, 12H), 1.54-1.70 (m, 4H), 3.76 (s, 4H), 4.14 (t, J = 6.7 Hz, 4H), 7.01 (dd, J = 5.1, 3.6 Hz, 2H), 7.13 (s, 2H), 7.17 (dd, J = 3.6, 1.1 Hz, 2H), 7.19 (s, 2H), 7.22 (dd, J = 5.1, 1.1 Hz, 2H); ^{13}C NMR (75 MHz, $CDCl_3$) δ 14.1, 22.7, 25.7, 28.7, 31.5, 35.9, 65.5, 124.1, 124.9, 126.9, 127.4, 128.0, 131.3, 131.6, 135.6, 136.3, 136.8, 170.8. ESI-MS m/z 697.2 [$(M+H)^+$ calcd for $C_{36}H_{41}O_4S_5^+$ 697.2].

Synthesis of PBCA-NPs

PBCA-NPs were synthesized by the miniemulsion process as described previously (41). Briefly, an oil-in-water emulsion was prepared by mixing a monomer oil phase with a water phase containing a PEG stabilizer (Brij®L23, Sigma-Aldrich). The monomer phase contained butyl cyanoacrylate (BCA, a kind gift from Henkel Loctite, Dublin, Ireland), a neutral oil as

co-stabilizer (Miglyol® 810N, kind gift from Cremer, Hamburg, Germany), a radical initiator (V65, Azobisdimetyl valeronitril, Wako, Osaka, Japan) and 0.5 wt% of the fluorescent dye(s). After emulsifying using sonication (Branson Ultrasonifier, Danbury, USA), Jeffamine®M-2070 (a polyetheramine with a 19-unit PEG chain, Huntsman Corporation, Salt Lake City, USA), was added to initiate the polymerization at the droplet surface. Polymerization was carried out at room temperature overnight. Potential unreacted monomer in the particle core was polymerized by increasing the temperature to 50°C for 8 h, activating free radical polymerization by V65. The particles were rinsed by extensive dialysis and stored in the dark at 4°C.

Synthesis of NEs

Oil-in-water NEs were prepared through a method based on swift evaporation of organic solvents as previously described (42). The amphiphilic lipids 1,2-disteraoyl-sn-glycero-3-phosphocholine (DSPC), cholesterol, and 1,2-disteraoyl-sn-glycerol-3-phosphoethanolamine-N-[methoxy(polyethylene glycol)-2000] (PEG–DSPE) (all from Avanti Polar Lipids, Alabaster, USA) were used at a molar ratio of 62:33:5. 0.5 mol% fluorophore and 2.6 mg of soybean oil per μmole of the amphiphilic lipid mixture were included. All components (typically 5 μmole of amphiphilic lipids) were combined in chloroform and dripped into 4.5 ml deionized H_2O at 72°C under vigorous magnetic stirring (1300 rpm). The chloroform evaporated instantly and the obtained crude emulsions were tip-sonicated for 20 min (Heat System Ultrasonics, W-225R, duty cycle 35%, 30 W and 20 kHz) in a water bath in order to maintain room temperature. The NEs were stored in the dark at 4°C until use.

Additional information about FCM experiments

The instrument was manufactured in 2009 and installed the same year. The optical filters used are original. The instrument has been serviced at a yearly basis. Before each experiment a quality control protocol was performed with to verify laser stability with Flow-check Pro Fluorospheres (A63493 - Beckmann Coulter).

The following lasers were used:

488nm default, 405nm, 561nm, 633nm

Photo multiplier tubes (PMT) were used as analyte detectors (FL2 582 nm, BP 15 nm; FL3 620 nm, BP 30 nm; FL6 660 nm, BP 20 nm; FL9 450 nm, BP 50 nm).

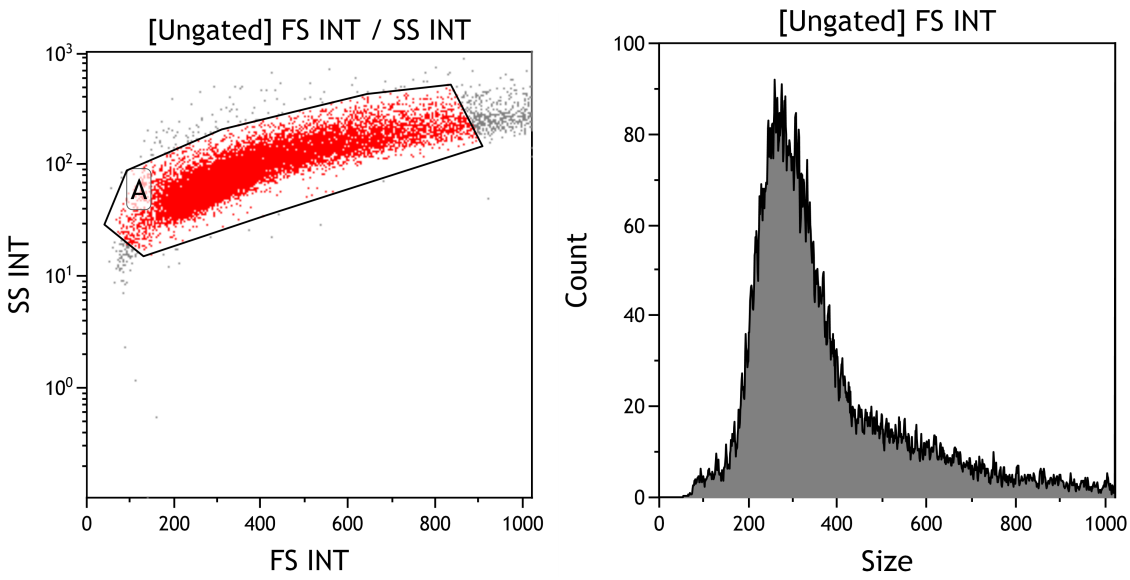

Figure 1: Example of a collection gate in the side-scatter versus forward-scatter dot plot and the corresponding histogram.

Table 1: Fluorescence intensity from PBCA-NPs, liposomes and NEs measured by spectrophotometer. Excitation/emission wavelengths were as follows: 561/620 nm for NR and

NR668, 405/450 nm for p-HTAH and p-HTAH, 633/668 nm for DiD and 561/596 nm for DiI. Average and standard deviation are shown, n = 2-4.

	NR	NR668	p-HTAM	p-HTAH	DiI	DiD
PBCA-NPs	44473±431	34178±745	9130±104	43422±341	44796±110	46272±400
NEs	46352±168	61432±2	8965±43	11026±158	44101±227	46005±32[a]
Liposomes	12995±413	3014±39	5600±3	5367±34	53110±162	21132±193
Water	315±11	315±11	4726±181	4726±181	174±6	719±41

[a]Measured at lower gain compared to the other DiD-NPs

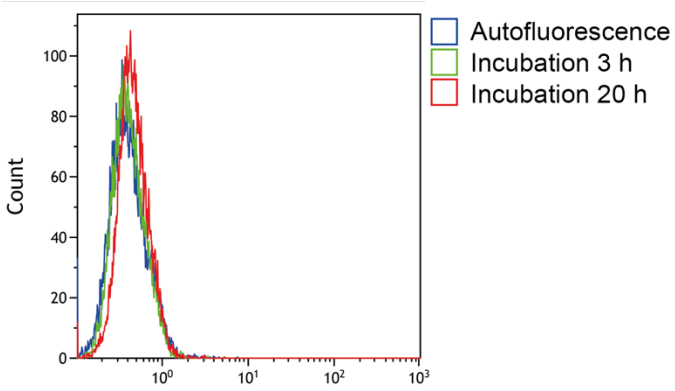

Figure 2: Flow cytometric histograms illustrating fluorescence from PC3 cells incubated with DiO-PBCA-NPs for 3 h and 20 h.

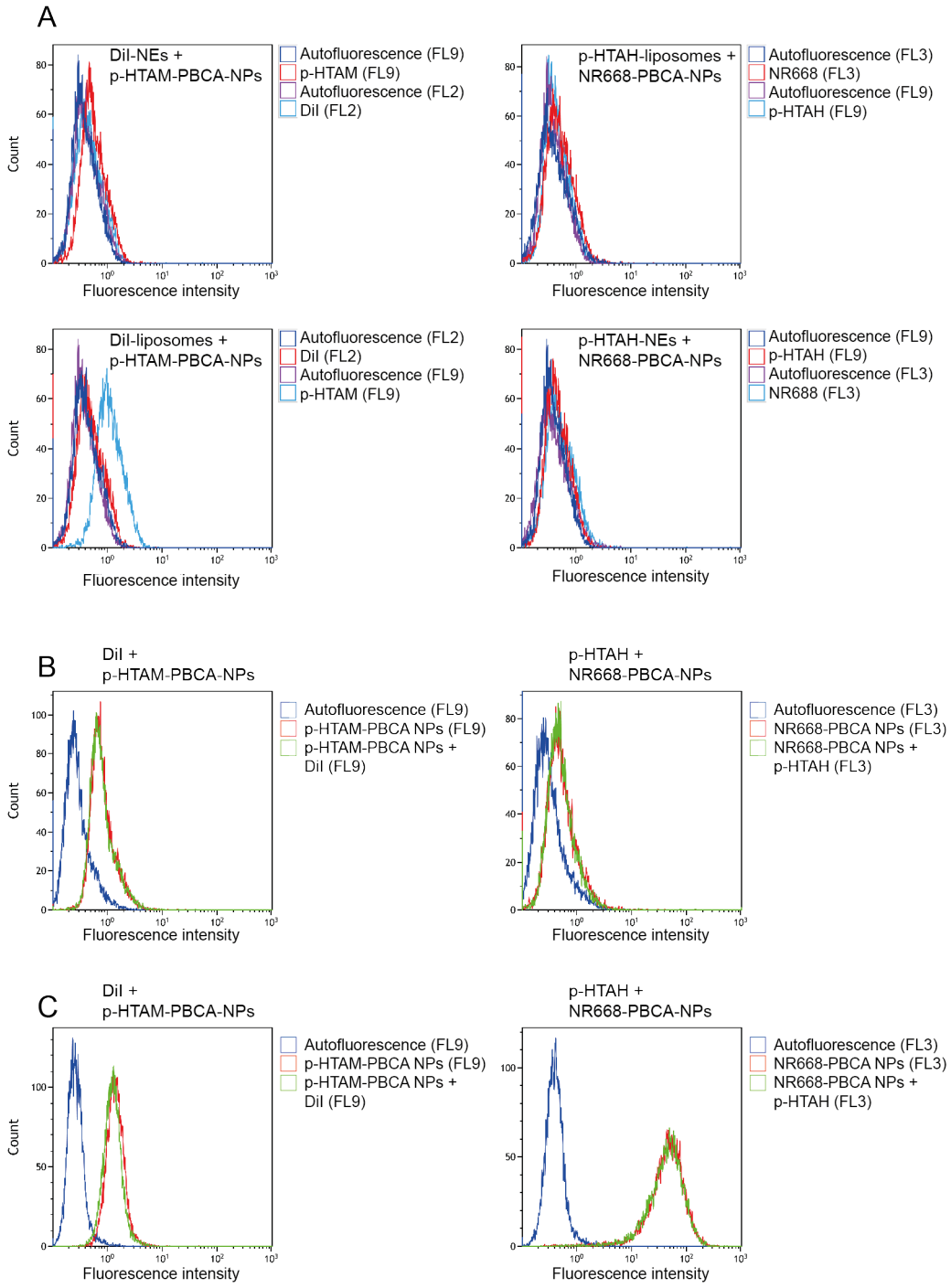

Figure 3: Flow cytometric histograms from co-incubation of NEs/liposomes with DiI/p-HTAH and PBCA-NPs with p-HTAM/NR668 in PC3 cells (A), and co-incubation of free dyes (DiI/p-HTAH) with PBCA-NPs with p-HTAM/NR668 in PC3 (B) and RBE4 cells (C).